New Paradigm for Design of High-Spin Organic Molecules: The Mechanism of Spin-Dependent Delocalization in Exchange-Coupled, Mixed-Valent Organic Species

Stefan Franzen* and David A. Shultz

Department of Chemistry, North Carolina State University, Raleigh, North Carolina 27695-8204

Received: December 2, 2002; In Final Form: March 10, 2003

A theory is developed to describe the electronic structure of mixed-valent, exchange-coupled organic biradicals. The phenomena described are analogous to those of spin-dependent delocalization observed in binuclear inorganic complexes in the sense that coupling of delocalized hole states favors a triplet state over a singlet state. However, the mathematical description of the delocalization is quite similar to Kramers' treatment of antiferromagnetic and ferromagnetic terms in metal oxides (*Physica* **1934**, *1*, 182). There is a similarity in that a delocalized orbital in the mixed-valent biradical anion can play the role of oxide in conventional superexchange. As in Kramers' theory, there are two terms that result from the analysis, a second-order term and a third-order term. However, the significance of the terms is different for delocalized magnetic orbitals than for the metal−bridge−metal system considered by Kramers. The computational chemistry shows that the third-order ferromagnetic term dominates for large dihedral angles, in agreement with previous experimental results. The mechanism presented suggests a new paradigm for the design of high-spin organic molecules.

Introduction

High-spin organic molecules ($S = 1$) have been the focus of intense study both from a theoretical perspective and as ligands to prepare molecule-based magnetic materials.[2−8] Most high-spin molecule design involves attaching paramagnetic functional groups to a π-system (a coupler) so as to achieve a cross-conjugated π-topology.[9,10] Such conncectivity gives nondisjoint NBMOs[11] that give rise to substantial exchange integrals that stabilize high-spin ground-states. For example, the structural features of trimethylenemethane and *meta*-xylylene form the basis of a plethora of high-spin molecules.[7,10,12] Up to the present time, this remains the only design paradigm for preparing high-spin molecules.

Certain mixed-valent metal complexes exhibit a spin−spin coupling mechanism for which there is no organic counterpart: double exchange, also called spin-dependent delocalization (SDD).[3,13−15] The salient feature of SDD is that the highest spin-multiplicity state is preferentially stabilized by electron delocalization, according to the transfer (resonance) integral, $|\beta|$. Despite the large number of mixed-valent organic compounds, only a few examples have molecular structures that enforce significant exchange coupling. Of these few, none exhibit either new coupling pathways or enhanced ferromagnetic coupling.[16−18] We feel that mixed-valent organic ligands hold a great deal of promise for new properties/behaviors,[19−23] particularly when the mixed-valent organic ligands have more than one unpaired electron.

Recently, we reported the first example of enhanced ferromagnetic coupling in a mixed-valent molecule that lacks an effective π-type ferromagnetic coupler ($[Na^+][(LZn)_3(SQ_2Cat)]^-$), formed from one-electron reduction of an antiferromagnetically coupled, isovalent triradical, $(LZn)_3(SQ_3)$.[22]

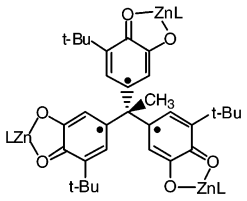

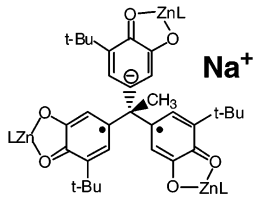

Herein, we develop a theory to account for the observed enhancement in ferromagnetic coupling in the mixed-valent biradical anion. Our theoretical treatment is supported by calculations on two model systems ($\mathbf{1}^{3\bullet}$ and $\mathbf{1}^{(2\bullet)-}$)—that serve as analogues of $(LZn)_3(SQ)_3$ and $[(LZn)_3(SQ_2Cat)]^-$, respectively—as well as a model biradical, $\mathbf{2}^{2\bullet}$.

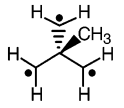

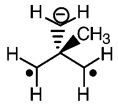

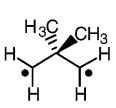

Methods

Model systems consisting of triradical $\mathbf{1}^{3\bullet}$ and biradical $\mathbf{2}^{2\bullet}$ shown in Figures 1 and 2, respectively, were studied using Hartree−Fock (HF) and post-HF methods. The role of electron correlation in determining the lowest spin state was tested using methods that included configuration interaction (CI) using three different methods. The first method is a CI calculation that includes singles, doubles, and triples (QCSDT).[24,25] The second method is a coupled cluster approach that also includes singles, doubles, and triples (CCSDT).[26−28] The third method used for comparison was a complete active space method CASSCF(4,6)

* Corresponding author.

10.1021/jp0276000 CCC: $25.00
Published on Web 05/06/2003

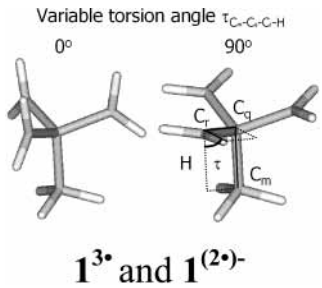

Figure 1. Model triradical ($\mathbf{1}^{3\bullet}$) and biradical anion ($\mathbf{1}^{(2\bullet)-}$). The unpaired electrons are on the three methylene groups. The p-orbital on each of the methylene groups serves as the atomic orbital in the orthogonalized magnetic orbital model. These molecules serve as models for the spin systems of the semiquinone species studied in ref 19.

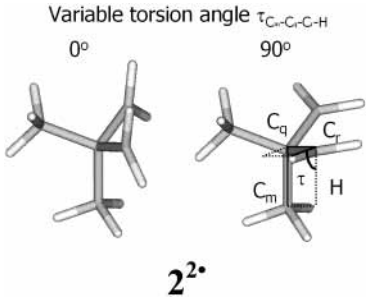

Figure 2. Model biradical ($\mathbf{2}^{2\bullet}$). The unpaired electrons are on the two methylene groups. The p-orbital on each of the methylene groups serves as the atomic orbital in the orthogonalized magnetic orbital model. The molecule serves as a model of a spin system of the semiquinone species studied in ref 19.

and CASSCF(6,10), where CASSCF(*N*,*M*) represents all possible electron configurations of *N* electrons in *M* active orbitals.[29−32] Comparison calculations were also run using density functional theory (B3LYP).[33,34] Gaussian98 was employed using a 6-31G** basis set.[35] CASSCF is not further discussed because initial agreement at the level of CASSCF(4,6) was not reproduced in the CASSCF(6,10) calculation (see Supporting Information). The DFT calculations are not discussed below because they too fail to accurately determine the spin gaps in any of the molecular models considered (see Supporting Information). While we cannot explain the failure of CASSCF or B3LYP calculations to obtain the correct spin ordering, we note that the weak coupling of organic radicals appears to be well-represented only using CI that includes singles, doubles, and triples (CISDT or coupled cluster CCSDT). Agreement with experiment is approached systematically in a trend from HF to CC(I)SD to CC(I)SDT. All calculations were carried out on the SGI/Cray Origin 2000 and IBM SP supercomputers at the North Carolina Supercomputer Center (NCSC).

The geometries of the radicals were systematically varied in order to determine conformational effects on the spin state energies, as shown in Figures 1 and 2. The figures define the dihedral angle $\tau_{C_m-C_q-C_r-H}$ and show the extreme dihedral angles used in the calculations. Calculations were carried out at four values of the $\tau_{C_m-C_q-C_r-H}$ dihedral angle: 0°, 30°, 60°, and 90°. The model calculations are intended to compare a neutral, isovalent biradical ($\mathbf{2}^{2\bullet}$) species shown in Figure 1 with a delocalized biradical anion ($\mathbf{1}^{(2\bullet)-}$) shown in Figure 2. The neutral biradical model for $\mathbf{2}^{2\bullet}$ has two electrons in p-orbitals orthogonal to the plane of the CH_2 groups. The biradical anion model for $\mathbf{1}^{(2\bullet)-}$ has four electrons delocalized over the three CH_2 groups shown in Figure 2. There are two structurally important limiting cases. For dihedral angles of $\tau_{C_m-C_q-C_r-H}$ = 0° and 90°, p-orbitals can have σ- and π-type interactions, respectively. The model shown in Figure 2 was also used for calculation of the triradical $\mathbf{1}^{(3\bullet)}$.

Results

Spin-State Ordering in a Biradical Model. We first calculate the singlet−triplet gap for a biradical using the active electron approximation for magnetic orbitals on centers 1 and 2, respectively. This treatment follows that presented by Kahn.[3] In an orthogonalized magnetic orbital picture for two centers, the wave functions are

$$\psi_+ = \frac{1}{\sqrt{2}}\{\phi_1 + \phi_2\} \qquad a \tag{1}$$

$$\psi_- = \frac{1}{\sqrt{2}}\{\phi_1 - \phi_2\} \qquad b \tag{2}$$

The Hamiltonian

$$H = h(1) + h(2) + 1/r_{12} \tag{3}$$

is used to calculate the one-electron integrals:

$$\alpha = \langle a(1)|h(1)|a(1)\rangle = \langle b(1)|h(1)|b(1)\rangle = \langle a(2)|h(2)|a(2)\rangle = \langle b(2)|h(2)|b(2)\rangle \tag{4}$$

$$\beta = \langle a(1)|h(1)|b(1)\rangle = \langle a(2)|h(2)|b(2)\rangle \tag{5}$$

$$j^0 = \langle a(1)a(2)|1/r_{12}|a(1)a(2)\rangle \tag{6}$$

$$j = \langle a(1)b(2)|1/r_{12}|a(1)b(2)\rangle \qquad \text{Coulomb} \tag{7}$$

$$k = \langle a(1)b(2)|1/r_{12}|a(2)b(1)\rangle \qquad \text{Exchange} \tag{8}$$

$$l = \langle a(1)b(2)|1/r_{12}|b(1)b(2)\rangle \qquad \text{Hybrid} \tag{9}$$

The singlet and triplet states of the ground configuration (GC) are

$$^1\Gamma_g(\text{GC}) = \frac{1}{\sqrt{2}}\{a(1)b(2) + a(2)b(1)\} \tag{10}$$

$$^3\Gamma_u(\text{GC}) = \frac{1}{\sqrt{2}}\{a(1)b(2) - a(2)b(1)\} \tag{11}$$

The first-order corrections to the energy become

$$E(^1\Gamma_g(\text{GC})) = 2\alpha + j + k \tag{12}$$

$$E(^3\Gamma_u(\text{GC})) = 2\alpha + j - k \tag{13}$$

and the singlet−triplet gap is the ferromagnetic contribution to the exchange parameter:

$$J_F = E(^1\Gamma_g(\text{GC})) - E(^3\Gamma_u(\text{GC})) = 2k \tag{14}$$

if one assumes zero overlap ($s = 0$) for orthogonalized magnetic orbitals following Kahn.[3] The triplet state is stabilized with respect to the singlet state due to the exchange interaction ($k > 0$). On the other hand, charge transfer between the two magnetic centers stabilizes the singlet. The charge-transfer configurations

(CTCs) are

$$^1\Gamma_g^+(\mathrm{CTC}) = \frac{1}{\sqrt{2}}\{a(1)a(2) + b(2)b(1)\} \quad (15)$$

$$^1\Gamma_g^-(\mathrm{CTC}) = \frac{1}{\sqrt{2}}\{a(1)a(2) - b(2)b(1)\} \quad (16)$$

The energies of the states are

$$E(^1\Gamma_g^+(\mathrm{CTC})) = 2\alpha + j^0 + k \quad (17)$$

$$E(^1\Gamma_g^-(\mathrm{CTC})) = 2\alpha + j^0 - k \quad (18)$$

Thus, the energy difference $E(^1\Gamma_g(\mathrm{GC})) - E(^1\Gamma_g^+(\mathrm{CTC})) = E(^3\Gamma_u(\mathrm{GC})) - E(^1\Gamma_g^-(\mathrm{CTC})) = j - j^0$. The singlet and triplet energies are changed by the second-order correction to the energies

$$E^{(2)}(^1\Gamma) = \frac{\langle ^1\Gamma_g(\mathrm{GC})|H|^1\Gamma_g^+(\mathrm{CTC})\rangle^2}{[E(^1\Gamma_g(\mathrm{GC})) - E(^1\Gamma_g^+(\mathrm{CTC}))]} \quad (19)$$

$$E^{(2)}(^3\Gamma) = \frac{\langle ^3\Gamma_u(\mathrm{GC})|H|^1\Gamma_g^-(\mathrm{CTC})\rangle^2}{[E(^3\Gamma_u(\mathrm{GC})) - E(^1\Gamma_g^-(\mathrm{CTC}))]} \quad (20)$$

We find that

$$\langle ^1\Gamma_g(\mathrm{GC})|H|^1\Gamma_g^+(\mathrm{CTC})\rangle = 2\beta + 2l \quad (21)$$

and

$$\langle ^3\Gamma_u(\mathrm{GC})|H|^1\Gamma_g^-(\mathrm{CTC})\rangle = 0 \quad (22)$$

The second-order term is an antiferromagnetic contribution to the exchange parameter due to the configuration interaction of CT states for orthogonalized magnetic orbitals ($s = 0$).

$$J_{\mathrm{AF}} = \frac{4(\beta + l)^2}{(j - j^0)} \quad (23)$$

The antiferromagnetic term can be as large as or larger than the ferromagnetic term, leading to a ground-state singlet in a biradical, since the exchange parameter is a sum of ferromagnetic and antiferromagnetic contributions:

$$\mathbf{J} = J_{\mathrm{F}} + J_{\mathrm{AF}} \quad (24)$$

Calculation of the Singlet−Triplet Gap in a Biradical Model. Biradical **2**$^{2\bullet}$ (Figure 1) was used as a model compound for the calculation of the relative energy of the singlet and triplet spin states. This energy gap provides a computational assessment of the intrinsic coupling ability of the sp^3 carbon in a biradical and can be compared to similar calculations on trimethylene and related biradicals.[9,36−39] To ensure that electron correlation has been adequately accounted for, the calculations were carried out at various levels for the biradical. If only singles and doubles are included, that is, QCISD or CCSD, there is still a triplet ground state in the biradical. It is first at the QCISDT or CCSDT level that we see a positive singlet−triplet gap energy (i.e., singlet lower in energy than the triplet) for the biradical case (Table 1). There is a conformational dependence to the magnitude of the singlet−triplet splitting, as shown in Table 1. The QCISDT and CCSDT calculations agree quite well except for the conformation with $\tau_{C_m-C_q-C_r-H} = 90°$. The QCISDT calculation predicts that a singlet state will be significantly stabilized in the π-type geometry for $\tau_{C_m-C_q-C_r-H} = 90°$ shown in Figure 1. On the other hand, the CCSDT calculation predicts that the singlet state will be destabilized at $\tau_{C_m-C_q-C_r-H} = 90°$ relative to $\tau_{C_m-C_q-C_r-H} = 0°$. It is evident from the above theory that the charge-transfer interaction is decisive for the stabilization of the singlet relative to the triplet. Although it is difficult to estimate the magnitude of the integrals for the simple model above in terms of the calculated energies, it is clear that orbital overlap plays a role in determining the relative contribution of J_F and J_{AF} to the spin state. The splitting is negative in sign (singlet state is lowest for all conformations) but has a maximum value (i.e. smallest negative value) near a dihedral angle of 30°, likely due to the reduced overlap between the p-orbitals on the neighboring CH_2 groups at this dihedral angle.[37]

TABLE 1: Energy of Neopentyl Radicals in eV as a Function of the $C_m-C_q-C_r-H$ Dihedral Angle[a]

		energy			
molecule	angle	HF	CCSD	CCSDT	QCISDT
2$^{2\bullet}$	0	−5303.15	−5325.55	−5326.73	−5326.75
singlet	30	−5302.54	−5325.22	−5326.56	−5326.55
	60	−5301.2	−5324.7	−5326.77	−5326.67
	90	−5302.34	−5325.16	−5326.57	−5327.28
2$^{2\bullet}$	0	−5305.71	−5325.92	−5326.51	−5326.52
triplet	30	−5305.75	−5325.95	−5326.55	−5326.55
	60	−5305.75	−5325.95	−5326.55	−5326.56
	90	−5305.73	−5325.93	−5326.53	−5326.54
1$^{3\bullet}$	0	−5287.98	−5307.18	−5307.75	−5308.62
doublet	30	−5287.98	−5307.13	−5307.67	−5308.54
	60	−5287.96	−5307.08	−5307.63	−5308.49
	90	−5287.96	−5307.09	−5307.64	−5308.49
1$^{3\bullet}$	0	−5287.9	−5306.99	−5307.54	−5308.35
quartet	30	−5288.02	−5307.11	−5307.65	−5308.49
	60	−5288.07	−5307.17	−5307.71	−5308.57
	90	−5288.02	−5307.12	−5307.66	−5308.52
1$^{(2\bullet)-}$	0	−5283.55	−5305.98	−5307.16	−5308.17
singlet	30	−5282.77	−5305.33	−5306.59	−5307.6
	60	−5280.97	−5303.77	−5305.27	−5306.22
	90	−5279.81	−5302.63	−5304.3	−5305.18
1$^{(2\bullet)-}$	0	−5285.22	−5305.56	−5306.22	−5307.12
triplet	30	−5285.22	−5305.5	−5306.16	−5307.09
	60	−5285.16	−5305.3	−5305.94	−5306.71
	90	−5285.15	−5305.65	−5306.35	−5307.19

[a] The $C_m-C_q-C_r-H$ dihedral angle is defined in Figure 1. The energy is reported for Hartree−Fock (HF) and three post-HF methods that include configuration interaction.

The model does provide a framework for interpretation of Hartree−Fock (HF) and post-HF calculations. The exchange interaction is included at the HF level, and charge transfer state contributions will only be evident if CI is included in the calculation. Table 2 shows that the sign and magnitude of the singlet−triplet gap depend greatly on electron correlation. At the HF level the triplet state is significantly lower in energy than the corresponding singlet state, consistent with a dominant contribution for the exchange interaction in J_F. It is evident that calculations that include higher electron correlation stabilize the singlet relative to the triplet, as predicted by the term J_{AF} in the orthogonalized magnetic orbital model given in eq 23.

Spin-State Ordering in a Triradical. The model triradical **1**$^{3\bullet}$ shown in Figure 2 provides a structure for calculation of the spin states of both the neutral (three-electron system) and anion (four-electron system). In an orthogonalized magnetic

TABLE 2: Spin Gaps of Neopentyl Radicals in eV as a Function of the $C_m-C_q-C_r-H$ Dihedral Angle[a]

		spin gap			
molecule	angle	HF	CCSD	CCSDT	QCISDT
$\mathbf{2}^{2\bullet}$	0	2.56	0.364	−0.214	−0.225
singlet−triplet gap	30	3.21	0.727	−0.0186	0.00299
	60	4.55	1.25	−0.215	−0.105
	90	3.39	0.769	−0.0434	−0.743
$\mathbf{1}^{3\bullet}$	0	−0.0816	−0.190	−0.218	−0.272
doublet−quartet gap	30	0.0413	−0.019	−0.0266	−0.0544
	60	0.113	0.0822	0.0792	0.0816
	90	0.0625	0.0302	0.0268	0.0272
$\mathbf{1}^{(2\bullet)-}$	0	1.68	−0.420	−0.941	−1.05
singlet−triplet gap	30	2.45	0.172	−0.435	−0.511
	60	4.184347	1.528841	0.668843	0.485248
	90	5.343282	3.016597	2.051835	2.013344

[a] The spin gaps calculated using the CCSDT and QCSIDT methods correspond to the plots in Figure 4.

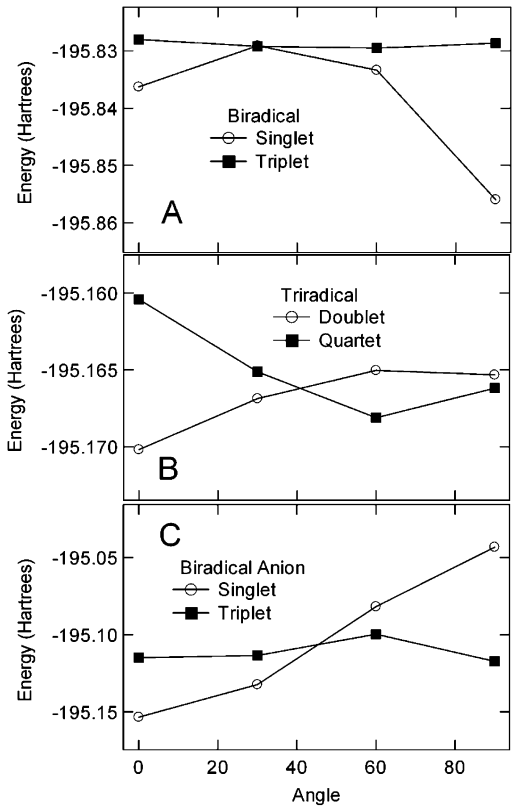

Figure 3. Comparison of the energy of the high-spin (quartet or triplet) and low-spin (doublet or singlet) states of three model molecules as a function of the $C_m-C_q-C_r-H$ dihedral angle shown in Figures 1 and 2 calculated using QCISDT.

orbital picture for three centers, the wave functions are

$$\psi_E = \frac{1}{\sqrt{2}}\{\phi_1 - \phi_3\} \qquad a \qquad (25)$$

$$\psi_E = \frac{1}{\sqrt{6}}\{\phi_1 - 2\phi_2 + \phi_3\} \qquad b \qquad (26)$$

$$\psi_A = \frac{1}{\sqrt{3}}\{\phi_1 + \phi_2 + \phi_3\} \qquad c \qquad (27)$$

The energies of the orbitals are α_A (α_c) and α_E (α_a and α_b),

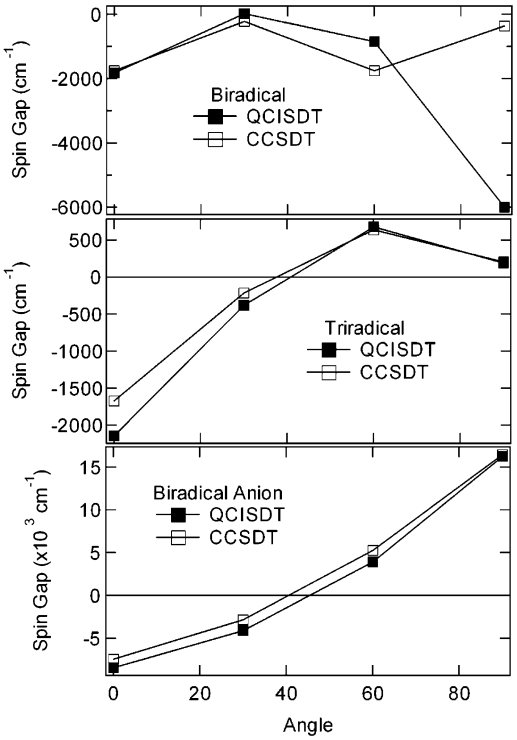

Figure 4. Calculated spin gap in inverse centimeters for three model molecules as a function of the $C_m-C_q-C_r-H$ dihedral angle shown in Figures 1 and 2. The definition of the spin gap is low spin minus high spin. **(**A**)** The singlet state is lower in energy than the triplet state for all dihedral angles, but is near zero at 30°. The QCISDT and CCSDT results differ qualitatively for the two molecules at a dihedral angle of $\tau = 90$ °. (B) The doublet−quartet spin gaps are negative for all dihedral angles $\tau < 50°$ in both calculations, indicating that the doublet state is lowest in energy for these energies. (C) Both calculations indicate that the singlet is lower in energy than the triplet when $\tau < 50°$ and the triplet is the ground state for $\tau > 50°$.

respectively. For a three-electron system, the doublet state will be the lowest in energy for either ordering of the orbitals unless the energy difference $\alpha_E - \alpha_A$ is less than the spin-pairing energy. The possible configurations and states are $\psi_E^4\psi_A^0$ (^{1}A); $\psi_E^3\psi_A^1$ (^{1}E, ^{3}E); and $\psi_E^2\psi_A^2$ (^{1}A, ^{3}A, ^{1}E). The lowest energy configurations emerge from post-HF calculations as discussed below.

Calculation of the Doublet−Quartet Gap in a Triradical Model. Triradical $\mathbf{1}^{3\bullet}$ (Figure 2) was used as a model compound for the calculation of the doublet−quartet spin gap. This energy gap provides a computational assessment of the intrinsic coupling ability of the sp^3 carbon in a triradical. Calculations at the highest level of correlation practical for the two methods QCISDT and CCSDT gave good agreement for the doublet−quartet spin gap (Figure 3). For $\mathbf{1}^{3\bullet}$ the spin gap is negative (indicating a doublet ground state) for $\tau_{C_m-C_q-C_r-H} < 40°$ (see Figure 4). For larger dihedral angles a quartet ground state is calculated for $\mathbf{1}^{3\bullet}$; however, the spin gap is quite small relative to the singlet−triplet gap for the biradical anion (see Figure 4).

Spin-State Ordering in a Biradical Anion Model. The orthogonalized magnetic orbitals approach can be applied for four electrons. The Hamiltonian is

$$H = h(1) + h(2) + h(3) + h(4) + 1/r_{12} + 1/r_{23} + 1/r_{34} + 1/r_{24} + 1/r_{14} + 1/r_{13} \qquad (28)$$

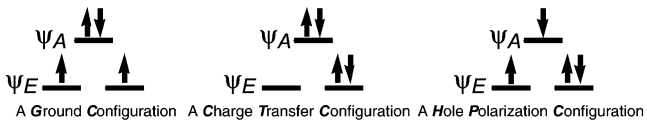

Figure 5. Electron configurations for the three orbital, four electron biradical anion: left, ground configuration; center, charge-transfer configuration; right, hole polarization configuration.

In the derivation of the intrinsic J_F and J_{AF} coupling, electrons 3 and 4 are passive:

$$^1\Gamma(\mathrm{GC}) = (2)^{-1/2}[a(1)b(2) + a(2)b(1)]c(3)c(4) \quad (29)$$

$$^3\Gamma(\mathrm{GC}) = (2)^{-1/2}[a(1)b(2) - a(2)b(1)]c(3)c(4) \quad (30)$$

and the ferromagnetic (J_F) and antiferromagnetic (via CTC involving SOMOs: J_{AF}) terms are the same as those derived above for the biradical, eqs 14 and 23, respectively. Orbitals *a* and *b* (eqs 25 and 26) in the biradical anion are not the same as *a* and *b* of the biradical **2**$^{2\bullet}$ (eqs 10 and 11), but they play the same role. In other words, *a* and *b* in the biradical anion generate the same ferromagnetic and antiferromagnetic terms. However, in the biradical *anion* there are also hole states that result from admixture of the totally symmetric orbital (Ψ_A) into the doubly degenerate pair (Ψ_E) via $\Psi_A \Rightarrow \Psi_E$ excited configurations (Figure 5).

In the following we consider the hole polarization (superexchange) terms that result in a ferromagnetic contribution. The hole polarization states (HPCs) are

$$^1\Gamma(HPC) = (2)^{-1}\{[c(3)b(2) + b(3)c(2)]a(1)a(4) + [c(3)a(1) + a(3)c(1)]b(2)b(4)\} \quad (31)$$

$$^3\Gamma(HPC) = (2)^{-1}\{[c(3)b(2) - b(3)c(2)]a(1)a(4) + [c(3)a(1) - a(3)c(1)]b(2)b(4)\} \quad (32)$$

$^1\Gamma$(HPC) could be either ^{1}A or ^{1}E, and $^3\Gamma$(HPC) is ^{3}A. The second-order HPC corrections have the form

$$E^{(2)}(^1\Gamma) = \frac{\langle ^1\Gamma(\mathrm{GC})|H|^1\Gamma(\mathrm{HPC})\rangle^2}{[E(^1\Gamma(\mathrm{GC})) - E(^1\Gamma(\mathrm{HPC}))]} \quad (33)$$

$$E^{(2)}(^3\Gamma) = \frac{\langle ^3\Gamma(\mathrm{GC})|H|^3\Gamma(\mathrm{HPC})\rangle^2}{[E(^3\Gamma(\mathrm{GC})) - E(^3\Gamma(\mathrm{HPC}))]} \quad (34)$$

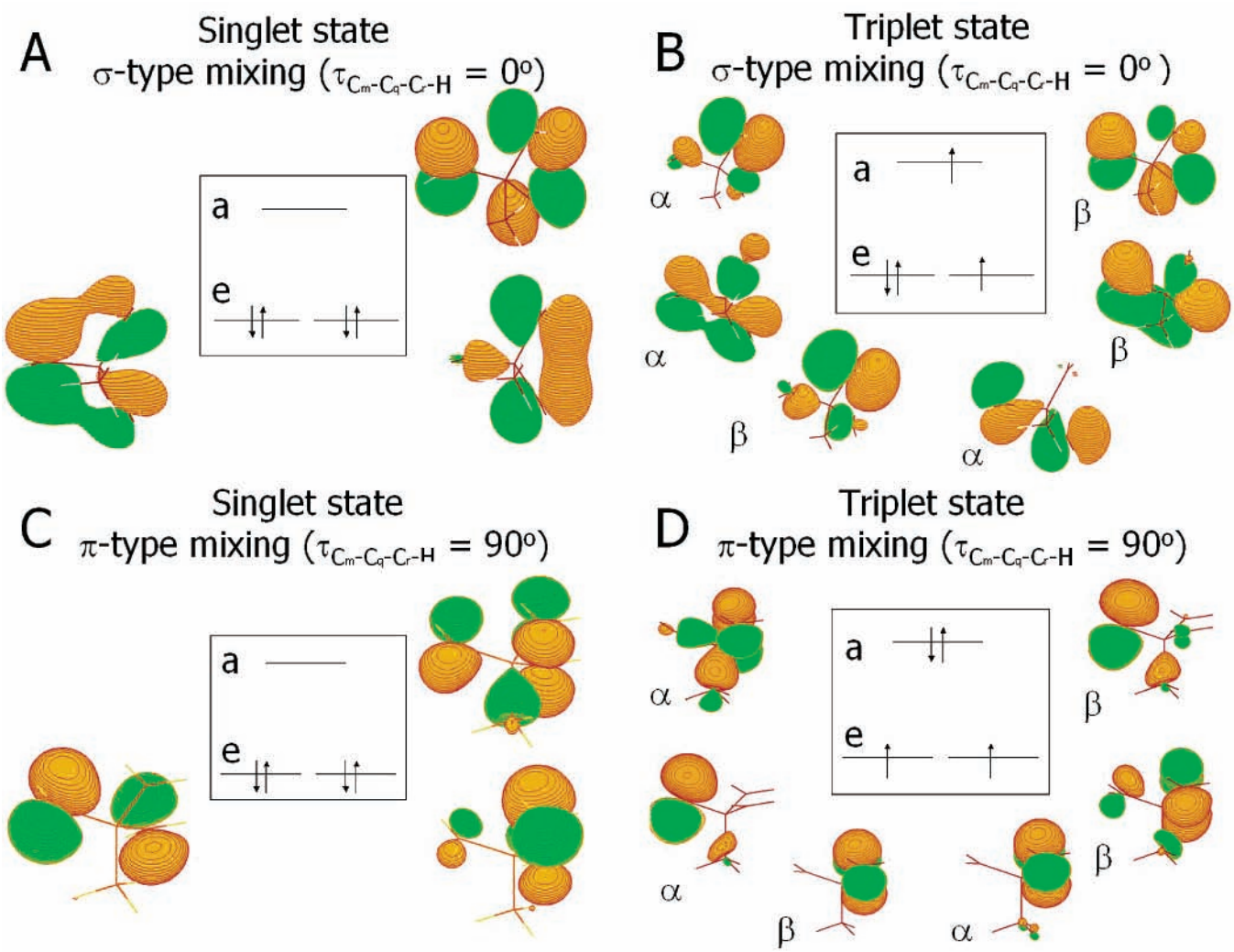

Figure 6. Orbital pictures for **1**($^{2\bullet}$)$-$: (A) singlet state with $\tau = 0°$; (B) triplet state with $\tau = 0°$; (C) singlet state with $\tau = 90°$; (D) triplet state with $\tau = 90°$.

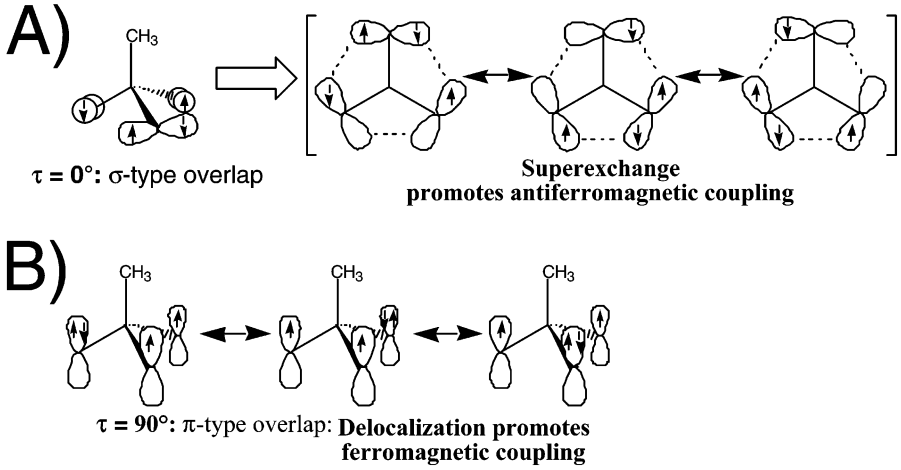

Figure 7. (A) Classic superexchange present in the hole polarization configuration of $\mathbf{1}^{(2\bullet)-}$. (B) Ferromagnetic exchange in the $\tau = 90°$ conformation of $\mathbf{1}^{(2\bullet)-}$.

Third-order HPC corrections have the form

$$E^{(3)}({}^1\Gamma) = \frac{\langle {}^1\Gamma(\mathrm{GC})|H|{}^1\Gamma(\mathrm{HPC})\rangle^2 \langle {}^1\Gamma(\mathrm{HPC})|H|{}^1\Gamma(\mathrm{HPC})\rangle}{[E({}^1\Gamma(\mathrm{GC})) - E({}^1\Gamma(\mathrm{HPC}))]^2} \quad (35)$$

$$E^{(3)}({}^3\Gamma) = \frac{\langle {}^3\Gamma(\mathrm{GC})|H|{}^3\Gamma(\mathrm{HPC})\rangle^2 \langle {}^3\Gamma(\mathrm{HPC})|H|{}^3\Gamma(\mathrm{HPC})\rangle}{[E({}^3\Gamma(\mathrm{GC})) - E({}^3\Gamma(\mathrm{HPC}))]^2} \quad (36)$$

This treatment differs from double exchange, where the higher multiplicity state is stabilized by the first-order correction, which is larger for the high-spin state than for the low-spin state, and is more similar to Kramers' superexchange.[1] In Kramers' derivation the second- and third-order terms are responsible for ferromagnetic and antiferromagnetic coupling, respectively.[1] The significance of the superexchange terms for delocalized magnetic orbitals (eqs 31 and 32) is different in that the second- and third-order terms result in antiferromagnetic and ferromagnetic contributions, respectively. Since the hole polarization configurations (HPCs) are higher in energy that the ground configurations (GCs), the energy denominator—and therefore the second-order HPC term given by eq 33—is negative and consequently antiferromagnetic. On the other hand, the third-order HPC term given by eq 35 is ferromagnetic, since here the energy denominator is positive. The triplet terms given in eqs 34 and 36 are both zero. These terms are significantly larger than any third-order correction that would involve CT configurations (Figure 5) because the HPC configurations are much closer in energy to the ground configurations.

Calculation of the Singlet−Triplet Gap in a Biradical Anion Model. CCSDT and QCISDT calculations predict that biradical anion $\mathbf{1}^{(2\bullet)-}$ (Figure 2) will have a triplet ground state for dihedral angles $\tau_{C_m-C_q-C_r-H} > 40°$. The triplet ground state for large dihedral angles arises due to the delocalization possible for π-type symmetry, as shown in the orbital diagrams in Figure 6, which gives the ordering of the energies of the SOMO, HOMO, and LUMO for four conformations of the biradical anion. The ordering of the MO energies in the QCISDT and CCSDT calculations corresponds closely with the orbital model proposed in eqs 25−27. Although the E symmetry orbitals are not rigorously degenerate in the calculations, they are close enough in energy that they can be represented as a doubly degenerate set, as shown in Figure 6. For $\tau_{C_m-C_q-C_r-H} = 0°$, a singlet ground state is predicted due to antiferromagnetic coupling that arises from the second-order HPC correction (eq 33) that dominates for σ-type orbital overlap. The singlet−triplet gap in $\mathbf{1}^{(2\bullet)-}$ is 4 times as large as that in $\mathbf{2}^{(2\bullet)}$ for this geometry due to the contribution of this term. For $\tau_{C_m-C_q-C_r-H} = 90°$ a triplet ground state is calculated for $\mathbf{1}^{(2\bullet)-}$ due to π-type orbital overlap that permits a third-order HPC correction to dominate. The superexchange theory developed above predicts that delocalized spin states will couple to give a triplet ground state, but only for the correct geometry.

Discussion

The phenomena described here are analogous to the phenomenon of spin-dependent delocalization observed in binuclear inorganic complexes in the sense that coupling of delocalized hole states favors a triplet state over a singlet. The mathematical description of the delocalization is quite similar to Kramers' treatment of antiferromagnetic and ferromagnetic terms in metal oxides.[1] There is a similarity in that the hole polarization state of $\mathbf{1}^{(2\bullet)-}$ can play the role of oxide in conventional superexchange, as suggested in Figure 7A.

There are two terms that result from the analysis of the admixture of hole polarization states. The second-order HPC term is antiferromagnetic, and the third-order HPC term is ferromagnetic. The computational chemistry shows that the third-order HPC ferromagnetic term dominates for large dihedral angles, that is, $\tau_{C_m-C_q-C_r-H} > 60°$. The delocalization that gives rise to the ferromagnetic term is illustrated in Figure 7B. The computational results for the antiferromagnetic exchange coupling in $\mathbf{1}^{3\bullet}$ and $\mathbf{2}^{2\bullet}$ are in accord with the previously reported experimental results for $(LZn)_3(SQ_3)$ and the protonated biradical $[(LZn)_3(SQ_2HCat)]$.[22] Most importantly, the mixed-valent species $\mathbf{1}^{(2\bullet)-}$ is a ground-state triplet, consistent with experimental results for $\mathbf{([Na^+][(LZn)_3(SQ_2Cat)]^-)}$.[22]

The application of Kramers-type superexchange to mixed-valent organic molecules forms the basis for a new paradigm for high-spin molecule design. To maximize the effect, one must maximize the ratio of ferromagnetic to antiferromagnetic contributions. By combining eqs 33 and 35, we get

$$\left|\frac{E^{(3)}}{E^{(2)}}\right| = \{|\langle^1\Gamma(\mathrm{GC})|H|^1\Gamma(\mathrm{HPC})\rangle^2\langle^1\Gamma(\mathrm{HPC})|H|^1\Gamma(\mathrm{HPC})\rangle \times [E(^1\Gamma(\mathrm{GC})) - E(^1\Gamma(\mathrm{HPC}))]\}/\{[E(^1\Gamma(\mathrm{GC})) - E(^1\Gamma(\mathrm{HPC}))]^2\langle^1\Gamma(\mathrm{GC})|H|^1\Gamma(\mathrm{HPC})\rangle^2|\} = \left|\frac{\langle^1\Gamma(\mathrm{HPC})|H|^1\Gamma(\mathrm{HPC})\rangle}{E(^1\Gamma(\mathrm{GC})) - E(^1\Gamma(\mathrm{HPC}))}\right| = \left|\frac{E(^1\Gamma(\mathrm{HPC}))}{E(^1\Gamma(\mathrm{GC})) - E(^1\Gamma(\mathrm{HPC}))}\right| \quad (37)$$

As can be seen in eq 37, the maximum ferromagnetic contribution can be achieved when $E(^1\Gamma(\mathrm{HPC}))$ approaches $E(^1\Gamma(\mathrm{GC}))$. This will tend to be the case for certain highly delocalized mixed-valent species. The important implication is that since the transfer integral, $|\beta|$, is often much greater than the exchange parameter, $|\boldsymbol{J}|$,[3] π-topologies that give disjoint NBMOs and low-spin ground states might give mixed-valent species (after oxidation or reduction) with high-spin ground states. In addition to an example having a saturated sp^3 exchange coupler previously reported by one of us,[22] we hypothesize that additional examples might include "doubly disjoint"[40−42] species, for example 1,3,5-tris(allyl)benzene and its analogues (Figure 8A).

We should point out that, in *nondisjoint* species, mixed-valency leads to weaker ferromagnetic coupling than that in the corresponding biradical. Consider the singlet−triplet gaps for the monoanion of benzene-1,3,5-triyl (Figure 8B, left) and *meta*-xylylene (Figure 8B, right).[43] These authors reasoned that the magnetic orbitals of the mixed-valent biradical anion were more disjointed than those of *meta*-xylylene, and therefore the inherent exchange integral is reduced compared to that of the parent *meta*-xylylene. This further suggests that the ferromagnetic effects of delocalization might best be found for doubly disjoint molecules, since their NBMOs are already disjoint.

Conclusions

We developed a theory for exchange coupling in mixed-valent organic biradicals. The study of inorganic double-exchanged systems has a clear antecedent in biology,[44,45] which motivates their study. However, the inorganic biological systems are quite complex, and in a fundamental sense, it is instructive to examine systems that lack d-orbitals. Along these lines, organic bi-/triradical systems are more amenable to both computational and experimental study than their inorganic counterparts. Computationally, we have shown that a high level of CI can be employed to obtain agreement of experiment and theory. In addition, structures of organic systems are quite easily manipulated so that one can systematically address factors such as geometry, substituents, and vibronic coupling that affect the spin gaps. Our theory combines elements of traditional double exchange and Kramers' treatment of exchange in metal oxides. The salient feature is that delocalization destabilizes low-spin states relative to high-spin states. The utility of this mechanism is that high-spin ground-state species can be created using a greater variety of couplers. We hope that our findings will lead to syntheses of interesting new molecules in which the effects of electron delocalization on electron spin alignment can be studied further.

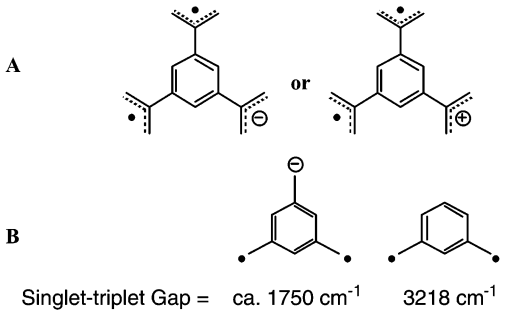

Figure 8.

Acknowledgment. This work was funded by the National Science Foundation (D.A.S.: Grant CHE-9910076) and start-up funds provided by North Carolina State University (S.F.). S.F. acknowledges support by North Carolina Supercomputer Center (NCSC) through the Visualization Initiative and a Faculty Account. D.A.S. thanks the Camille and Henry Dreyfus Foundation for a Camille Dreyfus Teacher−Scholar Award.

Supporting Information Available: The results for CASSCF and DFT calculations using the B3LYP functional, and derivations of the equations in the manuscript. This material is available free of charge via the Internet at http://pubs.acs.org.

References and Notes

(1) Kramers, H. A. *Physica* **1934**, *1*, 182.
(2) Lahti, P. M. *Magnetic Properties of Organic Materials*; Marcel Dekker: New York, 1999.
(3) Kahn, O. *Molecular Magnetism*; VCH: New York, 1993.
(4) Caneschi, A.; Gatteschi, D.; Sessoli, R.; Rey, P. *Acc. Chem. Res.* **1989**, *22*, 392.
(5) Miller, J. S.; Calabrese, J. C.; McLean, R. S.; Epstein, A. J. *Adv. Mater.* **1992**, *4*, 498.
(6) Luneau, D.; Laugier, J.; Rey, P.; Ulrich, G.; Ziessel, R.; Legoll, P.; Drillon, M. *J. Chem. Soc., Chem. Commun.* **1994**, 741.
(7) Iwamura, H.; Inoue, K.; Haymizu, T. *Pure Appl. Chem.* **1996**, *68*, 243.
(8) Iwamura, H.; Inoue, K. Magnetic Ordering in Metal Coordination Complexes with Aminoxyl Radicals. In *Magnetism: Molecules to Materials II. Molecule-Based Materials*; Miller, J. S., Drillon, M., Eds.; Wiley-VCH: New York, 2001; pp 61−108.
(9) Dougherty, D. A. *Acc. Chem. Res.* **1991**, *24*, 88.
(10) Rajca, A. *Chem. Rev.* **1994**, *94*, 871.
(11) Borden, W. T.; Davidson, E. R. *J. Am. Chem. Soc.* **1977**, *99*, 4587.
(12) Berson, J. A. *Diradicals*; Wiley: New York, 1982.
(13) Zener, C. *Phys. Rev.* **1951**, *82*, 403.
(14) Anderson, P. W.; Hasegawa, H. *Phys. Rev.* **1955**, *100*, 675.
(15) Girerd, J. J. *J. Chem. Phys.* **1983**, *79*, 1766.
(16) Nakamura, T.; Momose, T.; Shida, T.; Kinoshita, T.; Takui, T.; Teki, Y.; Itoh, K. *J. Am. Chem. Soc.* **1995**, *117*, 11292.
(17) Rajca, S.; Rajca, A. *J. Am. Chem. Soc.* **1995**, *117*, 9172.
(18) Sedó, J.; Ruiz, D.; VidalGancedo, J.; Rovira, C. J.; Bonvoisin, J.; Launay, J. P.; Veciana, J. *Adv. Mater.* **1996**, *8*, 748.
(19) Shultz, D. A.; Bodnar, S. H.; Kumar, R. K.; Kampf, J. W. *J. Am. Chem. Soc.* **1999**, *121*, 10664.
(20) Bencini, A.; Daul, C. A.; Dei, A.; Mariotti, F.; Lee, H.; Shultz, D. A.; Sorace, L. *Inorg. Chem.* **2001**, *40*, 1582.
(21) Shultz, D. A. *Polyhedron* **2001**, *20*, 1627.
(22) Shultz, D. A.; Kumar, R. K. *J. Am. Chem. Soc.* **2001**, *123*, 6431.
(23) Shultz, D. A. *Comments Inorg. Chem.* **2002**, *23*, 1.
(24) Krishnan, R.; Schlegel, H. B.; Pople, J. A. *J. Chem. Phys.* **1980**, *72*, 4654.
(25) Raghavachari, K.; Pople, J. A. *Int. J. Quantum Chem.* **1981**, *20*, 1067.
(26) Pople, J. A.; Krishnan, R.; Schlegel, H. B.; Binkley, J. S. *Int. J. Quantum Chem.* **1978**, *14*, 545.
(27) Pople, J. A.; Head-Gordon, M.; Raghavachari, K. *J. Chem. Phys.* **1987**, *87*, 5968.
(28) Bartlett, R. J.; Purvis, G. D. *Int. J. Quantum Chem.* **1978**, *14*, 561.
(29) Eade, R. H. E.; Robb, M. A. *Chem. Phys. Lett.* **1981**, *83*, 362.
(30) Frisch, M. J.; Ragazos, I. N.; Robb, M. A.; Schlegel, H. B. *Chem. Phys. Lett.* **1992**, *189*, 524.

(31) Hegarty, D.; Robb, M. A. *Mol. Phys.* **1979**, *38*, 1795.

(32) Yamamoto, N.; Vreven, T.; Robb, M. A.; Frisch, M. J.; Schlegel, H. B. *Chem. Phys. Lett.* **1996**, *250*, 373.

(33) Lee, C.; Yang, W.; Parr, R. G. *Phys. Rev. B* **1988**, *37*, 785.

(34) Miehlich, B.; Savin, A.; Stoll, H.; Preuss, H. *Chem. Phys. Lett.* **1989**, *157*, 200.

(35) Frisch, M. J.; Trucks, G. W.; Schlegel, H. B.; Scuseria, G. E.; Robb, M. A.; Cheeseman, J. R.; Zakrzewski, V. G.; Montgomery, J. A., Jr.; Stratmann, R. E.; Burant, J. C.; Dapprich, S.; Millam, J. M.; Daniels, A. D.; Kudin, K. N.; Strain, M. C.; Farkas, O.; Tomasi, J.; Barone, V.; Cossi, M.; Cammi, R.; Mennucci, B.; Pomelli, C.; Adamo, C.; Clifford, S.; Ochterski, J.; Petersson, G. A.; Ayala, P. Y.; Cui, Q.; Morokuma, K.; Malick, D. K.; Rabuck, A. D.; Raghavachari, K.; Foresman, J. B.; Cioslowski, J.; Ortiz, J. V.; Baboul, A. G.; Stefanov, B. B.; Liu, G.; Liashenko, A.; Piskorz, P.; Komaromi, I.; Gomperts, R.; Martin, R. L.; Fox, D. J.; Keith, T.; Al-Laham, M. A.; Peng, C. Y.; Nanayakkara, A.; Gonzalez, C.; Challacombe, M.; Gill, P. M. W.; Johnson, B. G.; Chen, W.; Wong, M. W.; Andres, J. L.; Head-Gordon, M.; Replogle, E. S.; Pople, J. A. *Gaussian 98 (Revision A.9)*; Gaussian, Inc.: Pittsburgh, PA, 1998.

(36) For a review of exchange coupling in 1,3-trimethylene-type biradicals, see the following and refs 37−39: Hoffmann, R. *J. Am. Chem. Soc.* **1968**, *90*, 1475.

(37) Goldberg, A. H.; Dougherty, D. A. *J. Am. Chem. Soc.* **1983**, *105*, 284.

(38) Getty, S. J.; Davidson, E. R.; Borden, W. T. *J. Am. Chem. Soc.* **1992**, *114*, 2085.

(39) Skancke, A.; Hrovat, D. A.; Borden, W. T. *J. Am. Chem. Soc.* **1998**, *120*, 7079.

(40) Matsumoto, T.; Ishida, T.; Koga, N.; Iwamura, H. *J. Am. Chem. Soc.* **1992**, *114*, 9952.

(41) Matsumoto, T.; Koga, N.; Iwamura, H. *J. Am. Chem. Soc.* **1992**, *114*, 5448−5449.

(42) Borden, W. T. Qualitative and Quantitative Predictions and Measurements of Singlet−Triplet Splittings in Non-Kekule Hydrocabon Diradicals and Heteroatom Derivatives. In *Magnetic Properties of Organic Materials*; Lahti, P. M., Ed.; Marcel Dekker: New York, 1999, Chapter 5.

(43) Wenthold, P. G.; Squires, R. R.; Lineberger, W. C. *J. Am. Chem. Soc.* **1996**, *118*, 475.

(44) Noodleman, L.; Lovell, T.; Liu, T. Q.; Himo, F.; Torres, R. A. *Curr. Opin. Chem. Biol.* **2002**, *6*, 259.

(45) Beinert, H.; Holm, R.; Munck, E. *Science* **1997**, *277*, 653.